Kinetics of Conformational Transitions in Polymers Containing Skeletal Double Bonds

Jeffrey Skolnick

Department of Chemistry, Louisiana State University, Baton Rouge, Louisiana 70803.
Received October 27, 1980

ABSTRACT: Multidimensional Kramers rate theory is employed to examine the influence exerted by double bonds on the kinetics of conformational transitions of single bonds in *trans*-polybutadiene and poly(*trans*-propenylene). For both molecules, a detailed discussion of the geometric and potential energy factors that determine the transition rates of the various types of single bonds is presented. Single bonds having next-nearest-neighbor double bonds are found to have mean transition rates half an order of magnitude smaller than that of a polymethylene-like molecule. Single bonds attached to double bonds are predicted to experience up to an order of magnitude enhancement in mean transition rate vis-à-vis polymethylene. Thus, it is concluded that double bonds through their modification of the torsional potential energy surface can produce important effects on the mechanism and rates of single-bond conformational transitions.

I. Introduction

Local motions in polymer molecules have been studied by a variety of experimental[1-3] and theoretical techniques[4-8] designed to elucidate the characteristics of such processes. In particular, computer simulations[9-12] have proven to be extremely useful in providing an understanding of a class of local relaxational modes, conformational transitions between rotational isomeric states. Guided by both simulation and experiment, a theory of conformational transitions applicable to polymers of arbitrary geometry and structure has recently been formulated.[13] In the context of this theoretical framework, we shall examine the influence exerted by the presence of double bonds on the time scale of conformational transitions of single bonds present in *trans*-polybutadiene and poly(*trans*-propenylene).

In previous work, a multidimensional version of Kramers' reaction rate theory was applied to treat the kinetics of conformational transitions in isolated chain molecules dissolved in a viscous solvent. Based on the observed apparent activation energy,[1,10] the theory assumed that conformational transitions proceed via single independent events and thus ignores the possibility of correlated transitions. The resultant reaction coordinate is a localized mode; consequently, the transition rate of a bond in an infinite polymer is finite.

In the current work, we investigate the effect of double bonds on the kinetics of conformational transitions in two representative polymer molecules, *trans*-polybutadiene (PBD) and poly(*trans*-propenylene) (PPP). While it is obvious the transition rate about a double bond itself is extremely small, intuitively it is not at all clear what the presence of a double bond does to the time scale of neighboring single-bond transitions. Does the torsional rigidity about the double bond diminish allowed motions of the transforming bond to the point where the time scale is significantly decreased? On the other hand, the double bond significantly changes the potential surface of nearest-neighbor single bonds: The barrier to rotation is smaller than in alkanes and the equilibrium conformations are entirely different.[14] Do these factors enhance or slow down the transition rate? It is the intent of this study to provide an estimate of the relative time scale of conformational transitions for molecules containing double bonds as compared to the analogous alkane-like molecule.

We have calculated transition rates of the central bond for three kinds of central bonds in 16-vertex linear-chain molecules. Sixteen-vertex chains are chosen because they reveal all the qualitative behavior of the infinite chain, in particular, the influence of tail orientation on transition rate and approximate time scale for conformational transitions, yet are sufficiently small that rapid generation and diagonalization of the interaction matrices are possible. To obtain the mean transition rate, $\bar{k}$, for a bond in the polymer molecule, we calculate $\bar{k}$ for the central bond in a 28-vertex molecule via a Monte Carlo procedure described previously.[13] $\bar{k}$ is calculated for all three types of central bonds discussed below.

The first two cases treat PBD-like molecules. In case A, the transforming central single bond is twice removed from a double bond and is denoted by bond type SS. The 16-atom molecule has the formula

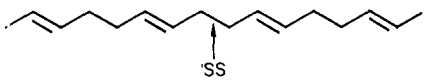

and shall be referred to as PBD-A. Case B has as its central bond a single bond attached to a double bond; single bonds attached to a double bond in PBD are designated type SSD. The molecular structure of the 16-vertex chain is

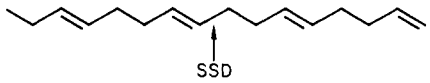

and shall be called PBD-B.

In case C we consider the kinetics of conformational transitions of a central single bond in a PPP-like molecule, for which the 16-vertex molecule has the formula

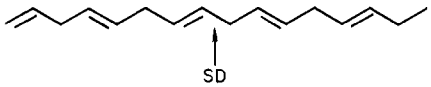

Single bonds of this type will be called type SD.

The organization of this paper is as follows. In section II a discussion of the molecular model used in the rate calculations is given. Subsequently, section III presents the results for the kinetics of conformational transitions in *trans*-polybutadiene and in poly(*trans*-propenylene). Finally, section IV summarizes the qualitative conclusions to be drawn from this work.

II. Polymer Model

Imagine an isolated polymer molecule immersed in a viscous solvent. Let the polymer consist of N vertices labeled 0 to $N-1$; each vertex represents a carbon backbone atom and attached substituent hydrogens. We shall assume that excluded-volume effects and hydrodynamic interactions are absent and that the backbone potential can be decomposed into independent bond stretching,

0024-9297/81/2214-0646$01.25/0

angle bending, and torsional contributions.

The molecules studied have $N - 1$ identical equilibrium bond lengths and $N - 2$ identical equilibrium bond angles. The angle bending and bond stretching potentials employed in our calculations may be found in ref 13.

We shall require three different torsional potentials, depending on whether the bond under consideration is a double bond, a single bond attached to a double bond (type SSD or SD), or a single bond having single-bond nearest neighbors (type SS).

For a double bond, we have taken the torsional potential $V_\phi^{\mathrm{d}}(\phi_i)$ to be of the form[15]

$$V_\phi^{\mathrm{d}}(\phi_i) = \frac{E_{\mathrm{d}}}{2}(1 - \cos \phi_i) \qquad \text{(II.1)}$$

E_{d} is taken to be 65 kcal/mol, the approximate value for a double bond in ethylene.[16]

Near the trans state, $\phi_i = 0$, we can expand

$$V_\phi^{\mathrm{d}}(\phi_i) = \tfrac{1}{2}\gamma_{\mathrm{t}}^{\mathrm{d}}\phi_i^2 \qquad \text{(II.2)}$$

Trans double bond states will be denoted by t_d.

The torsional potential of single bonds adjacent to double bonds, that is in bonds of the type R—C=C—C—R, is of the form[14]

$$V_\phi^{\mathrm{sd}} = \frac{E_{\mathrm{sd}}}{2}(1 - \cos (3\phi + \pi)) \qquad \text{(II.3)}$$

The potential minima occur at ±60° and at 180°. Following Flory,[14] we take E_{sd} to be 2.0 kcal/mol. The +60° and −60° states will be represented by g_s^+ and g_s^-, respectively. The cis state, at $\phi_i = 180°$, will be abbreviated as C.

In the vicinity of a cis state, we can approximate eq II.3 by

$$V_\phi^{\mathrm{sd}}(\phi_i) = \tfrac{1}{2}\gamma_{\mathrm{c}}(\phi_i - \pi)^2 \qquad \phi_i \text{ near } \pi \qquad \text{(II.4)}$$

Appendix A presents the Cartesian representation for $V_\phi^{\mathrm{sd}}(\phi_i)$ near a cis state.

Near g_s^+ or g_s^-

$$V_\phi^{\mathrm{sd}}(\phi_i) = \tfrac{1}{2}\gamma_{g_s}(\pi/3 \pm \phi_i)^2 \qquad \text{(II.5)}$$

in the neighborhood of g_s^- and g_s^+, respectively.

Finally, near the rotational barrier at $\phi_i^* = \pm 120°$ to a conformational transition

$$V_\phi^{\mathrm{sd}}(\phi_i) = E_{\mathrm{sd}}^* - \frac{\gamma_{\mathrm{sd}}^*}{2}\left(\frac{2\pi}{3} \pm \phi_i\right)^2 \qquad \text{(II.6)}$$

for ϕ_i near $-2\pi/3$ and $+2\pi/3$, respectively.

The rotational potential for a single bond, V_ϕ^{s}, having single-bond nearest neighbors is identical with that used in previous work for polymethylene-like molecules.[13] We can approximate V_ϕ^{s} by

$$V_\phi^{\mathrm{s}}(\phi_i) = \tfrac{1}{2}\gamma_{\mathrm{t}}\phi_i^2 \qquad \text{near trans} \qquad \text{(II.7)}$$

and

$$V_\phi^{\mathrm{s}}(\phi_i) = E_{\mathrm{g}} + \frac{\gamma_{\mathrm{g}}}{2}(2\pi/3 \pm \phi_i)^2 \qquad \text{(II.8)}$$

near gauche minus, g^-, and gauche plus, g^+, rotational states, respectively.

In the neighborhood of the trans–gauche barrier at ±60°

$$V_\phi^{\mathrm{s}}(\phi_i) = E_{\mathrm{s}}^* - \tfrac{1}{2}\gamma_{\mathrm{s}}^*(\phi \pm \pi/3)^2 \qquad \text{(II.9)}$$

The values of the parameters relating to the torsional potentials are compiled in Table I. Taken together, V_ϕ^{s}, V_ϕ^{sd}, and V_ϕ^{s} can be used to construct the torsional potential of molecules containing double bonds; in particular, *trans*-polybutadiene-like and poly(*trans*-propenylene)-like molecules are treated below.

Table I
Parameters Used in the Torsional Potentials[a]

parameter	value	unit
m	0.014	kg/mol
E_{d}	271.96	kJ/mol
	65.0	kcal/mol
$\gamma_{\mathrm{t}}^{\mathrm{d}}/m$	3.885×10^7	J/kg
E_{sd}^*	8.368	kJ/mol
	2.00	kcal/mol
γ_{c}/m	2.690×10^6	J/kg
γ_{g_s}/m	2.690×10^6	J/kg
γ_{sd}^*/m	2.690×10^6	J/kg
E_{s}^*	12.36	kJ/mol
	2.95	kcal/mol
γ_{t}/m	5.412×10^6	J/kg
γ_{g}/m	7.530×10^6	J/kg
γ_{s}^*/m	1.903×10^6	J/kg

[a] The mass is merely used to convert force constants into units of time, $\mathrm{J/(kg\ nm^2)} = \mathrm{ns^{-2}}$.

The general procedure for constructing the Cartesian representation of the harmonic approximation to the angle bending, bond stretching, and non-cis-torsional potentials may be found in Appendix A of ref 13.

III. Transition Rates in Molecules Containing Double Bonds

A. General Considerations. Suppose the jth bond in a molecule undergoes a conformational transition from some rotational state X to another rotational state X′; schematically, the process can be depicted as

$$\mathrm{PXQ} \rightarrow \mathrm{P'X'Q'} \qquad \text{(III.1)}$$

where P and Q and P′ and Q′, respectively, represent the orientation of the attached polymer tails before and after the transition. In previous work we have demonstrated that the rate transition for the process defined in eq III.1 is given by

$$k = \frac{|\lambda|}{2\pi\zeta}\left(\frac{\gamma_j}{\gamma_j^*}\right)^{1/2} \exp\left\{\frac{-E_j}{k_{\mathrm{B}}T}\right\} \qquad \text{(III.2)}$$

where $|\lambda|$ is the curvature of the path of steepest descent from the saddle point on the potential surface and is the negative eigenvalue of the potential energy matrix $\boldsymbol{W}$ defined in the vicinity of the saddle point.[17] ζ is the friction constant per polymer vertex and was taken to be 1.4×10^3 kg/ns. γ_j and γ_j^* refer to the potential curvature near X and near the barrier of the torsional potential of bond j, respectively. E_j is the barrier height. k_{B} is Boltzmann's constant and T is the absolute temperature. Equation III.2 can be rewritten as

$$k = f(j)|\lambda| \qquad \text{(III.3)}$$

Note that the tail geometry and size enter only in $|\lambda|$ and not in $f(j)$, which depends only on the properties of the bond j undergoing the conformational transition.

An increased understanding of the mechanism of conformational transitions emerges from a study of the localized mode, ρ^*, the negative eigenvector of $\boldsymbol{W}$ whose eigenvalue is λ.[17] The $3N$ Cartesian components of ρ^* are the displacements of the polymer vertices from the saddle point configuration in the direction of the path of steepest descents. Greater physical insight is obtained if ρ^* is converted into the corresponding bond stretching, angle

Table II
Localized Mode for $(t_dCtCt_dC)t(Ct_dCtCt_d)$ Initial State, 16-Vertex Chain[a]

j	D_{ϕ_i} $i = 8 \pm j$	D_{θ_i} $i = 8 + j$ or $7 - j$	D_{b_i} $i = 8 \pm j$
0	0.36	−0.016	−0.0013
1	−0.042	−0.014	−0.0028
2	0.012†	0.0018	−0.00042†
3	0.019	−0.00031	−0.0020
4	−0.049	−0.0064	−0.00088
5	−0.038	−0.0048	−0.0012
6	−0.0015†	0.00063	−0.000050†
7			−0.00040

[a] Superscript dagger denotes double bond.

Table III
Localized Mode for $(t_dCtCt_dg_s^+)t(g_s^+t_dCtCt_d)$ Initial State, 16-Vertex Chain[a]

j	D_{ϕ_i} $i = 8 \pm j$	D_{θ_i} $i = 8 + j$ or $7 - j$	D_{b_i} $i = 8 \pm j$
0	0.75	−0.031	−0.0030
1	−0.020	0.098	−0.0019†
2	−0.010†	−0.089	−0.0065
3	−0.039	−0.053	−0.00070
4	0.038	0.038	0.0054
5	0.021	0.014	−0.00062
6	−0.011†	−0.0090	−0.0033†
7			−0.00012

[a] Superscript dagger denotes double bond.

bending, and torsional modes, the technique of which is outlined below.

Let the overall motion of the polymer vertices be $\{d\rho_i^*\}$, subject to the constraint that

$$\sum_{i=1}^{N} |d\rho_i^*|^2 = b_0^2\, ds^2 \qquad \text{(III.4)}$$

Consequently, for a given total amount of motion $b_0\, ds$, the change in length of the ith bond is

$$db_i/b_0 = D_{b_i}\, ds \qquad \text{(III.5)}$$

The change in bond angle $d\theta_i$ is

$$d\theta_i = D_{\theta_i}\, ds \quad \text{(radians)} \qquad \text{(III.6)}$$

and the infinitesimal change in the ith torsional angle

$$d\phi_i = D_{\phi_i}\, ds \quad \text{(radians)} \qquad \text{(III.7)}$$

Explicit forms of D_{b_i}, D_{ϕ_i}, and D_{ϕ_i} in terms of the unit bond vectors defined at the saddle point may be found in Appendix C of Skolnick and Helfand.[13]

In all the calculations discussed below, both $|\lambda|$ and ρ^* were obtained numerically. The temperature was taken to be 371.12 K, so that $E_s^*/k_BT = 4.00$.

B. *trans*-Polybutadiene A: Type SS Bond Transition Rates. We consider the central-bond transition in a PBD-A molecule of the type

$$PtQ \rightarrow Pg^+Q \qquad \text{(III.8)}$$

Table II presents the bond stretching, angle bending, and torsional distortion displayed by the reaction coordinate near the saddle point for the transition

$$(t_dCtCt_dC)t(Ct_dCtCt_d) \rightarrow (t_dCtCt_dC)g^+(Ct_dCtCt_d) \qquad \text{(III.9)}$$

with $k = 0.38\ ns^{-1}$. Furthermore, Table III shows the decomposition of the localized mode into the torsional, angle bending, and bond stretching degrees of freedom accompanying

$$(t_dCtCt_dg_s^+)t(g_s^+t_dCtCt_d) \rightarrow (t_dCtCt_dg_s^+)g^+(g_s^+t_dCtCt_d) \qquad \text{(III.10)}$$

where $k = 1.05\ ns^{-1}$. Finally, Table IV displays the various D_{ϕ_i}, D_{θ_i}, D_{b_i} associated with

$$(t_dCtCt_dg_s^+)t(Ct_dCtCt_d) \rightarrow (t_dCtCt_dg_s^+)g^+(Ct_dCtCt_d) \qquad \text{(III.11)}$$

where $k = 0.64\ ns^{-1}$.

A detailed study of the localized mode of the transitions displayed in eq III.9–11, in addition to a large number of configurations not displayed here, leads to these qualitative conclusions:

B(1). In all cases the tail distortion acts to minimize the displacement of the nontransforming bonds while concomitantly maximizing D_{ϕ_s}. Whether or not $D_{\phi_{s\pm1}}$ and $D_{\phi_{s\pm2}}$ are positive or negative will depend on tail orientation; the resultant distortion acts to anneal the tails onto their original saddle point orientation.

B(2). Not surprisingly, the torsional distortion about a double bond is decreased relative to the value if a single bond were present.

B(3). As in the case of polymethylene-like molecules, the localized mode couples most effectively into the softest degrees of freedom, i.e., the torsional and to some extent the angle bending modes.

B(4). The presence of a cis rotational state immediately adjacent to the transforming bond introduces greater rigidity into that tail than if a g_s bond were present. This is reflected in the relative magnitudes of D_{ϕ_s} for the transformations shown in eq III.9–11. The placement of a cis rotational state at bond $i + 1$ relative to the transforming bond i causes bonds i and $i + 2$ to be nonparallel (although bonds i and $i + 2$ do lie in the same plane). Now the most effective torsional coupling that minimizes tail displacement results when bonds i and $i + 2$ are parallel. When a cis bond is located at $i + 1$, only a component of the bond rotation about bond $i + 2$ can restore the tail to its saddle point orientation. Consequently, cis bonds adjacent to transforming bonds give rise to tail rigidity in the direction of the reaction coordinate.

Table IV
Localized Mode for $(t_dCtCt_dg_s^+)t(Ct_dCtCt_d)$ Initial State, 16-Vertex Chain[a]

j	D_{ϕ_i} $i = 8 - j$	D_{ϕ_i} $i = 8 + j$	D_{θ_i} $i = 7 - j$	D_{θ_i} $i = 8 + j$	D_{b_i} $i = 8 - j$	D_{b_i} $i = 8 + j$
0	0.53		−0.013	−0.036	−0.0023	
1	−0.0095	−0.055	0.065	−0.029	−0.0028	−0.0037
2	−0.0086†	0.019†	−0.065	0.011	−0.0050†	0.00023†
3	−0.032	0.033	−0.041	0.0044	−0.0016	−0.0026
4	0.030	−0.074	0.026	−0.012	0.0035	−0.0018
5	0.017	−0.056	0.0086	−0.0075	−0.0010	−0.0015
6	−0.00088†	0.0023†	−0.0068	0.0016	−0.0025†	0.00024†
7					−0.00025	−0.00051

[a] Superscript dagger denotes double bond.

Table V
Relative Effects of Tail Orientation and Torsional Potential Curvature on the Transition Rate of the Central-Bond-Type SS t → g⁺ in a 16-Vertex Chain, $E_s^*/k_BT = 4$, of *trans*-Poly(butadiene)

initial state chain conformation	rate, ns^{-1}
$(\text{ttttt}g^+)t(g^+\text{ttttt})$	0.60
$(\text{ttttt}g_s^+)t(g_s^+\text{ttttt})$	1.49
$(\text{ttttt}_dg_s^+)t(g_s^+t_d\text{tttt})$	1.43
$(\text{ttt}g_s^+t_dg_s^+)t(g_s^+t_dg_s^+\text{ttt})$	0.82
$(tg_s^+tg_s^+t_dg_s^+)t(g_s^+t_dg_s^+tg_s^+t)$	0.90
$(t_dg_s^+tg_s^+t_dg_s^+)t(g_s^+t_dg_s^+tg_s^+t_d)$	0.90
$(\text{ttttt})t(\text{ttttt})$	5.05
$(\text{ttttt}_dt)t(tt_d\text{tttt})$	3.20
$(t_dt_stt_st_dt_s)t(t_st_dt_stt_st_d)$	3.82
$(t_dCtCt_dC)t(Ct_dCtCt_d)$	0.38

B(5). Relative to cis states, g_s conformations adjacent to transforming bonds produce relatively flexible tails. A g_s bond is 60° off a trans rotational state, the most flexible conformation. Thus while transition rates are significantly lower than trans (see below), g_s states nevertheless are more capable than C states of producing tail orientations that maximize D_{ϕ_s}, with a concomitant increase in transition rate.

B(6). When both a "flexible" and a "rigid" tail are present, the localized mode shifts over to the flexible tail with a resultant diminished tail torsional distortion relative to that of the central bond.

Quite a few effects on the transition rate of a central bond of type SS occur when considering PBD-A rather than polymethylene-like chains; consequently, we have investigated in Table V the relative contribution to k of the tail orientation and the magnitude of the torsional force constants. We begin by considering the influence of tail orientation and the presence of double bonds in gauche-type states. Note the enhanced transition rate of $(\text{ttttt}g_s^+)$ tails as compared to $(\text{ttttt}g^+)$ tails. The origin of this effect is clear. g_s^+ and g^+ states are 60° and 120° from trans, respectively. The closer the rotational state is to trans, the more flexible the attached tail becomes in the direction of the reaction coordinate. Observe the relatively small further decrease in k caused by the introduction of trans double bonds; the small decrease reflects, for g_s^+ first neighbors, the relative inability of even rotational states to the transforming bond to couple effectively into the reaction coordinate.

Let us now examine the transition rates for central bonds having trans or cis nearest neighbors. When bonds 7 and 9 are trans, introduction of trans double bonds results in a 40% reduction in k relative to single-bond nearest neighbors. When trans bonds are placed next to the transforming bond, bonds 6 and 10 couple strongly into the reaction coordinate. The increased potential energy to twist about a double bond (about a factor of 7) produces a significant diminution in transition rate. We now turn to the effect of torsional curvature of bonds 7 and 9 on the transition rate of the central bond. From Table I, it is apparent that $\gamma_c < \gamma_t$. To separate out the influence of tail orientation (cis vs. trans) as compared to curvature, we have calculated k for molecules having torsional curvature γ_c and trans potential minima, denoted by t_s. This gives a transition rate of 3.82 ns^{-1}. Note the striking reduction in k when cis rotational states are substituted for trans. In short, for type SS bonds, the dominant effect of double bonds is on the *tail* orientation. The single bond next to a double bond has a cis potential minimum and these orientations give rise to a significantly reduced k.

In Table VI, representative transition rates for central bonds of type SS in PBD-A are displayed. A study of these

Table VI
Representative Transition Rates of Bond 8 t → g⁺ of a Single-Bond-Type SS Having Single-Bond Nearest Neighbors in a 16-Vertex *trans*-Polybutadiene-like Molecule with $E_s^*/k_BT = 4$

initial state chain conformation	rate, ns^{-1}
$(t_dCtCt_dC)t(Ct_dCtCt_d)$	0.38
$(t_dCtCt_dg_s^+)t(Ct_dCtCt_d)$	0.64
$(t_dCtg_s^+t_dC)t(Ct_dCtCt_d)$	0.33
$(t_dg_s^+tCt_dC)t(Ct_dCtCt_d)$	0.46
$(t_dCtCt_dg_s^+)t(g_s^+t_dCtCt_d)$	1.05
$(t_dCtg_s^+t_dC)t(Ct_dg_s^+tCt_d)$	0.29
$(t_dg_s^+tCt_dC)t(Ct_dCtg_s^+t_d)$	0.51
$(t_dCtCt_dg_s^-)t(Ct_dCtCt_d)$	0.46
$(t_dCtg_s^-t_dC)t(Ct_dCtCt_d)$	0.38
$(t_dg_s^-tCt_dC)t(Ct_dCtCt_d)$	0.44
$(t_dCtCt_dg_s^-)t(g_s^-t_dCtCt_d)$	0.54
$(t_dCtg_s^-t_dC)t(Ct_dg_s^-tCt_d)$	0.37
$(t_dg_s^-tCt_dC)t(Ct_dCtg_s^-t_d)$	0.51
$(t_dCg^+Ct_dC)t(Ct_dCtCt_d)$	0.51
$(t_dCg^-Ct_dC)t(Ct_dCtCt_d)$	0.65
$(t_dCg^+Ct_dC)t(Ct_dCg^+Ct_d)$	0.63
$(t_dCg^-Ct_dC)t(Ct_dCg^-Ct_d)$	0.95
$(t_dg_s^-tg_s^-t_dg_s^-)t(g_s^-t_dg_s^-tg_s^-t_d)$	0.35
$(t_dg_s^-tg_s^-t_dg_s^+)t(g_s^-t_dg_s^-tg_s^-t_d)$	1.01
$(t_dg_s^-tg_s^-t_dg_s^+)t(g_s^+t_dg_s^-tg_s^-t_d)$	2.06
$(t_dg_s^-tg_s^+t_dg_s^+)t(g_s^+t_dg_s^+tg_s^-t_d)$	0.89
$(t_dg_s^+tg_s^-t_dg_s^+)t(g_s^+t_dg_s^-tg_s^+t_d)$	2.30
$(t_dg_s^+tg_s^-t_dg_s^-)t(g_s^-t_dg_s^-tg_s^+t_d)$	0.66
$(t_dg_s^+g^-g_s^+t_dg_s^+)t(g_s^+t_dg_s^+g^-g_s^+t_d)$	1.02
$(t_dg_s^+g^-g_s^+t_dg_s^+)t(g_s^+t_dg_s^+g^-g_s^+t_d)$	1.41
$(t_dg_s^+g^+g_s^+t_dg_s^+)t(g_s^+t_dg_s^+tg_s^+t_d)$	1.00
$(t_dg_s^+g^-g_s^+t_dg_s^+)t(g_s^+t_dg_s^+tg_s^-t_d)$	1.17
$(t_dg_s^-g^+g_s^-t_dg_s^-)t(g_s^-t_dg_s^-g^+g_s^-t_d)$	0.38
$(t_dg_s^-g^+g_s^-t_dg_s^-)t(g_s^-t_dg_s^-tg_s^-t_d)$	0.36

transition rates reveals these additional features:

BB(1). The approximate time scale for the transition is determined by the presence of g_s or C bonds next to the transforming rotational state. The placement of g_s bonds at positions odd to the transforming bond (at positions 5 and 11) gives slower transition rates and is analogous to previous observations for polymethylene-like molecules.

BB(2). g_s^+ states adjacent to the transforming bond tend to yield faster transition rates than g_s^-. The latter tails experience a greater displacement from the saddle point configuration than the former for a given amount of motion D_{ϕ_s}.

BB(3). Overall, we could expect the mean transition rate, $\bar{k}$, to be almost an order of magnitude slower for single bonds in PBD-A twice removed from double bonds when compared to single bonds in polymethylene. (See Table VI of ref 13.) The reduction in $\bar{k}$ arises chiefly from the presence of cis rotational state nearest neighbors.

To demonstrate the validity of observation BB(3), we have calculated the mean transition rate, $\bar{k}_{SS}$, for the central bond in a 28-vertex chain as follows:

$$\bar{k} = \sum_{\text{conf}} P_{\text{conf}} k_{\text{conf}} \qquad \text{(III.12)}$$

P_{conf} is the probability of observing the tails in a specified configuration, and k_{conf} is the transition rate of the central bond having the specified tail configurations and undergoing the t → g⁺ transition. The individual initial states were generated according to (III.13).

$$(tg_s^-t_dg_s^+tCt_dR_{ssd}R_{ss}X_{ssd}t_dX_{ssd})t(X_{ssd}t_dX_{ssd}R_{ss}R_{ssd}t_dCg^+ g_s^+t_dCg^-) \qquad \text{(III.13)}$$

R_{ss} indicates a g^-, g^+, or t state was statistically selected via a random number generator. R_{ssd} stands for a g_s^+, g_s^-, or C state chosen statistically. X_{ssd} indicates the selection of a C, g_s^-, or g_s^+ state with the associated proper equilibrium weighting in P_{conf}. All three rotational states are

Table VII
Localized Mode for $(Ct_dCtCt_d)C(tCt_dCtC)$ Initial State, 16-Vertex Chain[a]

	D_{ϕ_i}		D_{θ_i}		D_{b_i}	
j	$i = 8-j$	$i = 8+j$	$i = 7-j$	$i = 8+j$	$i = 8-j$	$i = 8+j$
0	−2.01		0.149	0.10	0.020	
1	0.069†	0.28	−0.044	−0.020	0.0093†	0.013
2	0.71	0.58	−0.017	−0.013	0.014	0.012
3	−0.26	−0.033†	0.038	0.032	0.0071	0.0045†
4	0.12	0.12	0.016	0.016	0.0041	0.0036
5	0.016†	0.094	−0.00015	−0.0014	−0.0014†	−0.0010
6	0.15	0.133	0.043	0.0032	0.0016	0.0015
7					0.00065	0.00065

[a] Superscript dagger denotes double bond.

Table VIII
Localized Mode for $(Ct_dCtCt_d)C(g^+Ct_dCtC)$ Initial State, 16-Vertex Chain[a]

	D_{ϕ_i}		D_{θ_i}		D_{b_i}	
j	$i = 8-j$	$i = 8+j$	$i = 7-j$	$i = 8+j$	$i = 8-j$	$i = 8+j$
0	−1.50		0.031	0.068	0.010	
1	0.039†	0.32	0.00082	−0.086	0.011†	0.0062
2	0.59	0.014	−0.012	−0.036	0.0060	0.018
3	−0.15	−0.033†	0.024	0.070	0.00091	0.012†
4	0.20	−0.19	0.017	0.033	0.0023	0.0074
5	0.015†	0.056	−0.0049	−0.025	−0.00066†	−0.0025
6	0.017	0.011	0.00097	0.0080	0.0012	0.0033
7					0.00072	0.0015

[a] Superscript dagger denotes double bond.

generated for each X_{ssd} bond. Therefore a total of 81 distinct tail configurations were generated and gave $\bar{k}_{SS}$ equal to 0.396 ns^{-1} at 371.12 K. This is to be contrasted with a $\bar{k}$ of 1.86 ns^{-1} for polymethylene-like chains. Consequently, observation 3 does indeed prove valid.

C. *trans*-Polybutadiene B: Type SSD Bond Transition Rates. This section examines transition rates for transformations in PBD-B type molecules. We begin with a discussion of transitions in 16-vertex molecules of the type

$$(Pt_d)C(XQ) \rightarrow (Pt_d)g_s^+(XQ) \qquad \text{(III.14)}$$

where X may be either t, g^+, or g^- in the molecule PBD-B. Observe that in the case of a $C \rightarrow g_s^+$ transition, the torsional angle is decreased; thus, reported values of D_{ϕ_8} will all be negative. Moreover, because one of the nearest neighbors is a trans rotational state and the other is either t, g^+, or g^-, we should expect the variation of k with tail orientation to be similar to that in alkanes. This is demonstrated below.

We consider in Table VII, the torsional distortion, angle bending, and bond stretching accompanying

$$(Ct_dCtCt_d)C(tCt_dCtC) \rightarrow (Ct_dCtCt_d)g_s^+(tCt_dCtC) \qquad \text{(III.15)}$$

with $k = 30.76$ ns^{-1}.

Similarly, the localized mode is presented in Table VIII for

$$(Ct_dCtCt_d)C(g^+Ct_dCtC) \rightarrow (Ct_dCtCt_d)g_s^+(g^+Ct_dCtC) \qquad \text{(III.16)}$$

with $k = 15.90$ ns^{-1}.

An analysis of the localized modes of these as well as a large number of additional configurations allows us to draw these conclusions:

C(1). As anticipated, trans states odd to the transforming bond lead to flexible tails vis-à-vis gauche (g) states.

C(2). The location of ϕ_8^* has a pronounced influence on the specific motion that maximizes D_{ϕ_8} subject to the constraint of minimal tail motion. Thus, if bond 9 is a trans state, the signs of D_{ϕ_9} and $D_{\phi_{10}}$ are the same rather than opposite, as would be observed in the case of an all-trans initial state chain. (See Table II of ref 13.) A detailed discussion of this effect may be found in Appendix B.

C(3). There is a diminished torsional distortion about double bonds.

C(4). The qualitative conclusions formulated for polymethylene localized modes are essentially applicable to type SSD single bonds.

Certainly one of the most striking features of the transitions depicted in eq III.15 and III.16 is the greatly increased transition rate in type SSD bonds relative to type SS bonds.

Possible sources of the enhanced transition rate are as follows:

CC(1). The curvature about the potential minima is less for single bonds of type SSD than of type SS; e.g., γ_c/m and γ_{g_s}/m are equal to 2.6×10^6 J/kg while $\gamma_t/m = 5.412 \times 10^6$ J/kg and $\gamma_g/m = 7.53 \times 10^6$ J/kg. Therefore it costs less energy to distort out tails having type SSD single bonds and $|\lambda|$ should increase.

CC(2). The curvature about the torsional potential maximum of SSD bonds is larger than in SS bonds; γ_{sd}^*/m equals 2.69×10^6 J/kg as compared to a γ_s^*/m of 1.903×10^6 J/kg. This acts to further speed up the transition.

CC(3). The barrier height is lower in type SSD bonds; $E_{sd}^*/k_BT = 2.70$ compared to $E_s^*/k_BT = 4.00$.

CC(4). However, $\gamma_c/\gamma_{sd}^* = 1$ while $\gamma_t/\gamma_s^* = 2.84$. The square root of these ratios reflects an entropic contribution to the transition rate. In this case, bonds of type SS are favored to give an increased transition rate.

CC(5). The presence of double bonds themselves should slow down the transition rate somewhat.

Taking observations CC(3) and CC(4) together gives the prefactor f, defined in eq III.3, a value for SSD bonds of 264.28 ns^{-1} vs. an f of 122.9 ns^{-1} for type SS single bonds. Thus bonds of type SSD experience a net factor of 2.15 rate increase vis-à-vis SS bonds due to barrier and entropic considerations.

Table IX
Relative Influence of Tail Orientation, Torsional Potential Curvature, and Barrier Height on the Transition Rate of the Central-Bond C → g_s^+ Transition in a 16-Vertex Chain of *trans*-Polybutadiene Type B ($E_{sd}^*/k_BT = 2.705$)

initial state chain conformation	rate, ns^{-1}	comments
$(g_s^+t_dg_s^+tg_s^+t_d)C(tg_s^+t_dg_s^+tg_s^+)$	36.46	polybutadiene-like molecule
$(g_s^+t_dg_s^+tg_s^+t_d)C(tg_s^+t_dg_s^+tg_s^+)$	22.51	g_s^+ force constants γ_{gs} have been set equal to γ_g
$(g^+t_dg^+tg^+t_d)C(tg^+t_dg^+tg^+)$	19.47	γ_g force constants used
$(g^+t_dg^+tg^+t_d)t(tg^+t_dg^+tg^+)$	10.84	$f = (1/2\pi\beta)(\gamma_c/\gamma_{sd}^*)^{1/2} \times \exp\{-E_{sd}^*/k_BT\}$; curvature of torsional potential near barrier = γ_s^*
$(g^+t_dg^+tg^+t_d)t(tg^+t_dg^+tg^+)$	5.04	$f = (1/2\pi\beta)(\gamma_t/\gamma_s^*)^{1/2} \times \exp\{-E_s^*/k_BT\}$; curvature of torsional potential = γ_s^*
$(g_s^+tg_s^+tg_s^+t)C(tg_s^+tg_s^+tg_s^+)$	41.91	

Table X
Representative Transition Rates of Bond 8 C → g_s^+ of a Single Bond next to a Double Bond in a 16-Vertex *trans*-Polybutadiene-like Molecule ($E_{sd}^*/k_BT = 2.705$)

initial state chain conformation	rate, ns^{-1}
$(Ct_dCtCt_d)C(tCt_dCtC)$	30.76
$(Ct_dCtCt_d)C(g^+Ct_dCtC)$	15.90
$(Ct_dCtCt_d)C(g^-Ct_dCtC)$	14.15
$(Ct_dCg^+Ct_d)C(tCt_dCtC)$	30.56
$(Ct_dCtCt_d)C(tCt_dCg^+C)$	30.31
$(Ct_dCtg_s^+t_d)C(tCt_dCtC)$	34.53
$(Ct_dg_s^+tCt_d)C(tCt_dCtC)$	29.48
$(g_s^+t_dCtCt_d)C(tCt_dCtC)$	31.02
$(Ct_dCtCt_d)C(tg_s^+t_dCtC)$	30.80
$(Ct_dCtCt_d)C(tCt_dg_s^+tC)$	29.18
$(Ct_dCtCt_d)C(tCt_dCtg_s^+)$	30.97
$(g_s^+t_dCtCt_d)C(tCt_dCtg_s^+)$	31.23
$(Ct_dg_s^+tCt_d)C(tCt_dg_s^+tC)$	27.79
$(Ct_dCtg_s^+t_d)C(tg_s^+t_dCtC)$	36.06
$(g_s^+t_dg_s^+tg_s^+t_d)C(tg_s^+t_dg_s^+tg_s^+)$	36.46
$(g_s^+t_dg_s^+tg_s^+t_d)C(g^+g_s^+t_dg_s^+tg_s^+)$	12.52
$(g_s^+t_dg_s^+g^+g_s^+t_d)C(g^+g_s^+t_dg_s^+tg_s^+)$	8.74
$(g_s^+t_dg_s^+g^-g_s^+t_d)C(tg_s^+t_dg_s^+tg_s^+)$	31.23
$(g_s^+t_dg_s^+tg_s^+t_d)C(tg_s^+t_dg_s^+g^+g_s^+)$	37.01
$(g_s^+t_dg_s^+tg_s^+t_d)C(tg_s^+t_dg_s^+g^-g_s^+)$	36.13
$(g_s^+t_dg_s^+tg_s^+t_d)C(g^-g_s^+t_dg_s^+tg_s^+)$	14.15
$(g_s^-t_dg_s^-tg_s^-t_d)C(g^-g_s^-t_dg_s^-tg_s^-)$	13.02
$(g_s^-t_dg_s^-g^+g_s^-t_d)C(g^-g_s^-t_dg_s^-tg_s^-)$	7.30
$(g_s^-t_dg_s^-tg_s^-t_d)C(tg_s^-t_dg_s^-tg_s^-)$	27.74

The relative role of effects CC(1) to CC(5) are assessed in Table IX.

Table X provides representative transition rates for conformational transitions of the kind depicted in eq III.14. An examination of the rates results in these qualitative conclusions:

CCC(1). The approximate transition rate is established by the conformation of the nearest neighbors to the transforming bond. The presence of a trans double bond guarantees the flexibility of at least one attached tail in the direction of the localized mode. In the XQ tail, when X is trans, k is about a factor of 2 faster than when X is g^+ or g^-.

CCC(2). Whether an even bond to ϕ_8 is g_s or C, both result in fairly flexible tail configurations. Observe that a tCt_d combination of rotational states makes bond $i + 4$ parallel to and collinear with bond i; when $i = 8$, tail motion is consequently diminished.

Table XI
Representative Transition Rates of Bond 8 C → g_s^+ in a Poly(*trans*-propenylene)-like Molecule ($E_{sd}^*/k_BT = 2.705$)

initial state chain conformation	rate, ns^{-1}
$(CCt_dCCt_d)C(Ct_dCCt_dC)$	12.48
$(g_s^+Ct_dCCt_d)C(Ct_dCCt_dg_s^+)$	11.21
$(Cg_s^+t_dCCt_d)C(Ct_dCg_s^+t_dC)$	12.19
$(CCt_dg_s^+Ct_d)C(Ct_dg_s^+Ct_dC)$	10.16
$(CCt_dCg_s^+t_d)C(g_s^+t_dCCt_dC)$	18.49
$(CCt_dCCt_d)C(g_s^+t_dCCt_dC)$	17.32
$(CCt_dCCt_d)C(Ct_dg_s^+Ct_dC)$	10.80
$(CCt_dCCt_d)C(Ct_dCg_s^+t_dC)$	11.88
$(CCt_dCCt_d)C(Ct_dCCt_dg_s^+)$	12.27
$(CCt_dCg_s^+t_d)C(Ct_dCCt_dC)$	12.55
$(CCt_dg_s^+Ct_d)C(Ct_dCCt_dC)$	11.69
$(Cg_s^+t_dCCt_d)C(Ct_dCCt_dC)$	12.78
$(g_s^+Ct_dCCt_d)C(Ct_dCCt_dC)$	11.44
$(g_s^-g_s^-t_dg_s^-Ct_d)C(Ct_dg_s^-g_s^-t_dg_s^-)$	10.02
$(g_s^-g_s^-t_dg_s^-g_s^-t_d)C(Ct_dg_s^-g_s^-t_dg_s^-)$	11.51
$(g_s^-g_s^-t_dg_s^-g_s^-t_d)C(g_s^-t_dCg_s^-t_dg_s^-)$	17.12
$(g_s^-g_s^-t_dg_s^-g_s^-t_d)C(g_s^-t_dg_s^-Ct_dg_s^-)$	17.60
$(g_s^-g_s^-t_dg_s^-g_s^-t_d)C(g_s^-t_dg_s^-g_s^-t_dC)$	19.08
$(g_s^-g_s^-t_dg_s^-Ct_d)C(g_s^-t_dg_s^-g_s^-t_dg_s^-)$	15.10
$(g_s^-g_s^-t_dCg_s^-t_d)C(g_s^-t_dg_s^-g_s^-t_dg_s^-)$	14.09
$(g_s^-Ct_dg_s^-g_s^-t_d)C(g_s^-t_dg_s^-g_s^-t_dg_s^-)$	16.88
$(Cg_s^-t_dg_s^-g_s^-t_d)C(g_s^-t_dg_s^-g_s^-t_dg_s^-)$	18.22
$(g_s^-g_s^-t_dg_s^-g_s^-t_d)C(g_s^-t_dg_s^-g_s^-t_dg_s^-)$	19.62
$(g_s^+g_s^+t_dg_s^+g_s^+t_d)C(g_s^+t_dg_s^+g_s^+t_dg_s^+)$	22.30
$(g_s^+g_s^+t_dg_s^+g_s^+t_d)C(g_s^+t_dg_s^+g_s^+t_dg_s^+)$	27.11
$(g_s^-g_s^-t_dg_s^-g_s^+t_d)C(g_s^-t_dg_s^-g_s^-t_dg_s^-)$	21.25
$(g_s^-g_s^-t_dg_s^+g_s^-t_d)C(g_s^-t_dg_s^-g_s^-t_dg_s^-)$	16.03
$(g_s^-g_s^+t_dg_s^-g_s^-t_d)C(g_s^-t_dg_s^-g_s^-t_dg_s^-)$	18.60
$(g_s^+g_s^-t_dg_s^-g_s^-t_d)C(g_s^-t_dg_s^-g_s^-t_dg_s^-)$	17.70

CCC(3). The transition rates of the central bond of type SSD in PBD are about an order of magnitude faster than those observed for 16-vertex alkane-like molecules.

To further examine conclusion CCC(3), we have obtained the mean transition rate $\bar{k}_{SSD}$ for the central bond of type SSD, C → g_s^+, in a 28-vertex PBD-like molecule via a procedure similar to that outlined in section B. The representative initial state conformations were taken to be of the form (III.17), where R_{ssd}, R_{ss}, and X_{ssd} have been

$$(Cg^-Ct_dg_s^+tR_{ssd}t_dR_{ssd}X_{ss}X_{ssd}t_d)C(X_{ss}X_{ssd}t_dR_{ssd}R_{ss}g_s^-t_dg_s^+ g^+Ct_dg_s^-) \quad \text{(III.17)}$$

previously defined and X_{ss} indicates the selection of a g^+, g^-, or t state with the correct equilibrium weighting in P_{conf}. The mean transition rate, $\bar{k}_{SSD}$, calculated on the basis of 81 sampled configurations using eq III.12 was 19.62 ns^{-1}. This is to be contrasted with the transition rate of 1.86 ns^{-1} obtained for single bonds in polymethylene. Clearly then, the theory predicts an order-of-magnitude increase in transition rate for SSD-type bonds in *trans*-polybutadiene vis-à-vis single bonds in alkane-like polymers.

D. Poly(*trans*-propenylene): Type SD Bond Transition Rates. We now turn to conformational transitions of bond type SD in poly(*trans*-propenylene). First, to understand the influence of attached tail configuration on transition rate, we consider conformational transitions of the central bond in a 16-vertex molecule. The process may be depicted schematically as

$$(Pt_d)C(YQ) \rightarrow (Pt_d)g_s^+(YQ) \quad \text{(III.18)}$$

Y may assume the values g_s^+, g_s^-, or cis.

No new concepts are necessary to understand the calculated transition rates and associated localized modes; rather transitions of SD bonds can be understood in terms of ideas developed in sections III.B and III.C. We therefore omit a detailed discussion of the localized mode and im-

mediately examine representative transition rates, as shown in Table XI.

These conclusions are apparent:

D(1). A trans double bond located adjacent to the transforming state guarantees that at least one attached tail is flexible. Combined with a larger prefactor (chiefly due to the difference in barrier heights), transition rates are about half an order of magnitude faster than in alkanes.

D(2). The presence of a g_s rotational state gives a somewhat enhanced transition rate vis-à-vis a g state.

For example, the type SSD bond in the initial state $(Ct_dCtCt_d)C(g^+Ct_dCtC)$ has a transition rate of 15.90 ns^{-1} while $(CCt_dCCt_d)C(g_s^+t_dCCt_dC)$ has a transition rate of 17.32 ns^{-1}. A g_s^+ conformation lies closer to a trans conformation than does a g^+ conformation. Thus the attached tail is more flexible in the direction of the reaction coordinate in the former case than in the latter.

D(3). The introduction of cis rotational states as a nearest neighbor to ϕ_s results in an appreciable reduction in transition rate due to geometric factors discussed previously (see observation B(4)). The geometric rigidity introduced by cis rotational states reduces the transition rate by a factor of 2–3 relative to type SSD bonds in PBD.

To determine the mean transition rate $\bar{k}_{SD}$ in a PPP polymer molecule, we have calculated $\bar{k}_{SD}$ for the central bond in a 28-vertex chain for the $C \rightarrow g_s^+$ transition. The representative initial state configuration used was (III.19).

$$(Cg_s^-t_dg_s^+Ct_dR_{ssd}R_{ssd}t_dX_{ssd}X_{ssd}t_d)C(X_{ssd}t_dX_{ssd}R_{ssd}t_dR_{ssd}g_s^-t_dg_s^+Ct_dg_s^+) \quad \text{(III.19)}$$

In all a total of 81 distinct configurations were sampled, and employing eq III.12, a value of $\bar{k}_{SD}$ equal to 8.15 ns^{-1} was found. Thus, transitions are about a factor of 4.4 faster in PPP than in alkanes. The reduction in transition rate of type SD bonds in PPP relative to type SSD bonds in PBD is caused to a large extent by the presence of cis nearest neighbors in PPP.

E. Effect of a More Realistic Potential on Calculated Transition Rates. We now examine the effect of the introduction of a more realistic equilibrium chain geometry and potential on the qualitative conclusions of this section. Let us consider the bond stretching potential first. The substitution of the correct equilibrium value for the bond length of a double bond (0.134 nm as opposed to 0.153 nm) will result in the following: It will increase the effective angle bending force constant, γ_θ, in the potential matrices by a factor of at most 1.14. As will be shown elsewhere, the decrease in transition rate due to this increase in γ_θ is negligible. Furthermore, the increase in effective torsional force constant of the double bond and nearest- and next-nearest-neighbor single bonds will be at most a factor of 1.30. As demonstrated in Tables V and IX, k is fairly insensitive to the value of γ_d. Furthermore, an increase in the effective torsional curvature of the transforming bond of bond types SSD and SD along the reaction coordinate speeds up the transition rate and acts to more than offset the decrease in k arising from greater effective torsional curvature near the bottom of the torsional potential wells. (See Appendix A of Skolnick and Helfand for values of the effective torsional curvature.[13]) Finally, an increase in γ_b accompanying the introduction of the double bond should also exert a fairly minor influence on transition rates. In short, the introduction of a more realistic bond potential should leave the qualitative conclusions formulated previously intact.

The introduction of the correct equilibrium values (θ_i = 55°) for bond angles associated with double bonds will have two effects: First, it will modify the reaction coordinate by stretching the chain out. (The end-to-end vector increases.) This will tend to decrease the rate of transition. Second, it increases the effective curvature of the torsional potentials near the minima and the maxima. To provide an estimate of the magnitude of these effects consider the transition

$$(Ct_dCtCt_d)C(tCt_dCtC) \rightarrow (Ct_dCtCt_d)g_s^+(tCt_dCtC) \quad \text{(III.20)}$$

when all the bond angles are tetrahedral, k = 30.76 ns^{-1}. Setting all the θ_i equal to 55° and letting the force constants remain unchanged yield k = 24.07. However, introducing the corrected values for the effective torsional force constants gives k of 53.53 ns^{-1}, a *net increase* of 74%, thereby showing the important influence of the magnitude of the negative torsional curvature of the transforming bond on the transition rate. Of course, in the real chain the increase in transition rate will be somewhat smaller.

Table XII
Transition Rate and Localized Mode Torsional Displacement in $(t_st_st_st_st_st_st_s)X^*(t_st_st_st_st_st_st_s)$ as a Function of ϕ^* with E_s^*/k_BT = 2.705 and $\gamma^* = \gamma_{sd}^*$

ϕ^*, deg	D_{ϕ_s}	$D_{\phi_{s\pm1}}$	$D_{\phi_{s\pm2}}$	rate, ns^{-1}
60.0	2.01	2.77×10^{-1}	-6.57×10^{-2}	30.132
80.0	2.21	1.58×10^{-1}	-7.38×10^{-1}	49.941
90.0	2.29	7.57×10^{-2}	-7.48×10^{-1}	56.058
95.0	2.33	3.24×10^{-2}	-7.48×10^{-1}	57.587
97.5	2.35	1.08×10^{-2}	-7.46×10^{-1}	57.916
98.5	2.35	2.27×10^{-3}	-7.44×10^{-1}	57.963
98.75	2.357	1.30×10^{-4}	-7.44×10^{-1}	57.9673
98.765	2.357	1.68×10^{-6}	-7.44×10^{-1}	57.9675
98.77	2.357	-4.10×10^{-5}	-7.44×10^{-1}	57.9676
98.78	2.357	-1.26×10^{-4}	-7.44×10^{-1}	57.9676
99.0	2.358	-2.00×10^{-3}	-7.44×10^{-1}	57.9684
100.0	2.365	-1.05×10^{-2}	-7.43×10^{-1}	57.941
117	2.44	-1.40×10^{-1}	-6.89×10^{-1}	49.437

Overall then, the implementation of a more realistic chain potential will have the following results: For single bonds with next-nearest-neighbor double bonds, the transition rate will be somewhat greater, although it is expected that $\bar{k}_{SS}$ will still be slower than the corresponding transition rate in alkanes, $\bar{k}_a$. With respect to single bonds of type SD and SSD, $\bar{k}_{SD}$ and $\bar{k}_{SSD}$ will be somewhat increased, therefore further reinforcing the qualitative conclusions that $\bar{k}_{SSD}$ and $\bar{k}_{SS}$ are significantly larger than $\bar{k}_a$.

IV. Conclusions

In the context of multidimensional Kramers rate theory, the effect of double bonds on the conformational transition rate of nearest- and next-nearest-neighbor single bonds has been investigated. Due to modification of the potential surface caused by the presence of a double bond, single bonds twice removed from the double bond (SS) may have cis nearest neighbors; cis bonds induce rigidity into the tail attached to the transforming bond. Consequently, the SS bonds experience a *reduction* in transition rate vis-à-vis an alkane chain. On the other hand, single bonds directly attached to a double bond, such as in *trans*-polybutadiene (SSD) and in poly(*trans*-propenylene) (SD), are predicted to experience an *enhanced* transition rate k over their alkane counterparts. The lowered barrier to rotation and the presence of at least one trans neighboring bond are primarily responsible for the increased value of k.

The present study points out the necessity for examining the effects of tail orientations, potential energy curvature near potential extrema, and barrier heights when calculating transition rates. On the basis of our study, *trans*-polybutadiene should have local relaxational rates that

vary on two time scales: one characteristic of type SS and one characteristic of type SSD bonds. We note in passing that NMR studies of polydienes in the melt have revealed the presence of two local relaxational processes[18] which may depend on backbone geometry.[19] However, at this time the relationship between local relaxational mechanisms in polymer melts and those postulated here for dilute solutions is unclear. Finally, an isolated molecule of poly(*trans*-propenylene) is expected to exhibit considerable local dynamic flexibility when compared to the corresponding alkane molecule. Experimental measurements and computer simulations are clearly required to test these predictions on the effects of double bonds on the kinetics of conformational transitions.

Acknowledgment. The author thanks Professor A. Holtzer for originally suggesting the problem and Professor W. Stockmayer for providing references for NMR studies of diene polymers. Acknowledgment is made to the donors of the Petroleum Research Fund, administered by the American Chemical Society, and the Louisiana State University Council on Research for partial support of this research.

Appendix A. Cartesian Representation of the Torsional Potential near Cis States

In the following, the reader will find it helpful to consult Appendix A of Skolnick and Helfand.[13]

In the vicinity of a cis state, we can expand the torsional potential as

$$V_\phi(\phi_i) = V_\phi(\pi) + \tfrac{1}{2}V_{\phi_i}'(\pi - \phi_i)^2 \qquad \text{(A.1)}$$

Prime denotes differentiation with respect to cos ϕ_i evaluated at $\phi_i = \pi$. We desire the ϕ_i in terms of the Cartesian displacements. It proves useful to consider

$$\sin\phi_i = \frac{-(\mathbf{b}_{i-1} \times \mathbf{b}_i) \times (\mathbf{b}_i \times \mathbf{b}_{i+1})}{|\mathbf{b}_i|^2|\mathbf{b}_{i-1}||\mathbf{b}_{i+1}| \sin\theta_{i-1} \sin\theta_i} \qquad \text{(A.2)}$$

with $\mathbf{b}_i$ the ith bond vector.

Now

$$\mathbf{b}_i = \mathbf{b}_i^\circ + \rho_i - \rho_{i-1} \qquad \text{(A.3)}$$

where $\mathbf{b}_i^\circ$ is the equilibrium value of $\mathbf{b}_i$ and ρ_i is the displacement of the ith vertex from its equilibrium position.

Substitution of eq A.3 into eq A.2, to terms of lowest order in displacements from equilibrium positions, gives

$$\sin\phi_i = -[(\mathbf{e}_i^\circ \times \mathbf{e}_{i+1}^\circ)\cdot(\rho_{i-1} - \rho_{i-2}) + (\mathbf{e}_{i+1}^\circ \times \mathbf{e}_{i-1}^\circ)\cdot(\rho_i - \rho_{i-1}) + (\mathbf{e}_{i-1}^\circ \times \mathbf{e}_i^\circ)\cdot(\rho_{i+1} - \rho_i)]/b_0 \sin^2\theta_0 \qquad \text{(A.4)}$$

provided that all the equilibrium values of the bond lengths and bond angles are the same.

Defining $\phi_i = \pi + \delta_i$ and placing the resultant expression for δ_i into eq A.1, we can cast eq A.1 into a form similar to that of the non-trans-torsional potential, i.e.

$$V_\phi(\phi_i) = V_\phi(\pi) + \frac{V_\phi'}{2b_0^2 \sin^4\theta_0} \times [\mathbf{B}_i\cdot(\rho_{i-1} - \rho_{i-2}) + \mathbf{O}_i\cdot(\rho_i - \rho_{i-1}) + \mathbf{F}_i\cdot(\rho_{i+1} - \rho_i)]^2 \qquad \text{(A.5)}$$

with

$$\mathbf{B}_i = \mathbf{e}_i^\circ \times \mathbf{e}_{i+1}^\circ \qquad \mathbf{O}_i = \mathbf{e}_{i+1}^\circ \times \mathbf{e}_{i-1}^\circ \qquad \mathbf{F}_i = \mathbf{e}_{i-1}^\circ \times \mathbf{e}_i^\circ$$

In passing we note that the form of eq A.5 is also applicable for ϕ_i near trans. For $\phi_i = 0$, $\mathbf{e}_{i-1} = \mathbf{e}_{i+1}$; $\mathbf{O}_i = 0$ and $\mathbf{B}_i = -\mathbf{F}_i$, and eq A.4 gives eq A.21 of Skolnick and Helfand.[13]

Appendix B. Torsional Displacements in the Localized Mode as a Function of ϕ^*

Let us consider the values of $D_{\phi_8\pm_1}$ and $D_{\phi_8\pm_2}$ as a function of ϕ^*, the location of the barrier to rotation corresponding to the configuration

$$(t_s t_s t_s t_s t_s t_s)X^*(t_s t_s t_s t_s t_s t_s) \qquad \text{(B.1)}$$

Here X* is the conformation of the transforming bond whose torsional angle at the barrier is ϕ^*. As usual, t_s refers to a trans bond with torsional force constant γ_c. The transforming bond has force constant γ_c and γ_{sd}^* near the bottom of the well and the top of the rotational barrier, respectively. The results for the transition rate and D_{ϕ_i}, i = 6–10, are displayed in Table XII.

We call attention to the following features of Table XII:

(1) $D_{\phi_8\pm_1}$ changes sign at about 98.765°.

(2) Observe the almost constant value of $D_{\phi_8\pm_2}$ as $D_{\phi_8\pm_1}$ goes from 2.27×10^{-3} to -2×10^{-3}. Moreover, as $D_{\phi_8\pm_1}$ goes to zero, the torsional motion of the attached tails is decreased relative to D_{ϕ_8} with a concomitant increase in transition rate.

(3) In all cases $D_{\phi_8\pm_2}$ remains negative and acts to restore the tail to the original saddle point configuration.

The question naturally arises as to why $D_{\phi_8\pm_1}$ changes sign as ϕ^* goes from 60° to beyond 98.765°? The answer is straightforward, provided that one recognizes the nature of the reaction coordinate: The localized mode is in the direction of the path of steepest descents from the saddle point on the potential energy surface and maximizes the rotational motion of the transforming bond for a given overall amount of motion of the vertices.

Between 0 and 90° an increase in $d\phi_8$ causes vertices 6 and 9 with their attached tails to move away from vertices 7 and 8. In order to maximize D_{ϕ_8}, subject to a given total amount of motion, there must be compensating distortions of the neighboring rotational angles. The motion of $D_{\phi_8\pm_2}$ is apparent; it must occur in the counterclockwise direction. Due to the orientation of the tails, a negative value of $D_{\phi_8\pm_1}$ will produce strong coupling to the angle bonding degrees of freedom. A positive value of $D_{\phi_8\pm_1}$ does not experience this additional cost in potential energy and is a natural consequence of the motion of vertices 7 and 8. Thus $D_{\phi_8\pm_1}$ greater than zero is the direction of choice and lies on the path of steepest descents.

Consider now ϕ^* greater than 90°. An increase in $d\phi_8$ causes vertex 6 to move away from vertices 7 and 8 and vertex 9 to move toward vertives 7 and 8. This imparts a sort of twisting motion to the transforming bond. As ϕ^* increases beyond 90° the coupling to the angle bending degrees of freedom caused by $D_{\phi_8\pm_1}$ less than zero diminishes. Moreover, the twisting motion corresponds to a negative $D_{\phi_8\pm_1}$. At some point, the resistance to a negative value of $D_{\phi_8\pm_1}$ caused by angle bending forces is precisely compensated for by the natural tendency of the transforming bond to twist, to minimize tail motion, and $D_{\phi_8\pm_1}$ is identically zero. Any further increase in ϕ^* produces negative values of $D_{\phi_8\pm_1}$ associated with the path of steepest descents.

References and Notes

(1) Morawetz, H. *Acc. Chem. Res.* **1970**, *3*, 354.
(2) Valeur, B.; Monnerie, L. *J. Polym. Sci., Polym. Phys. Ed.* **1976**, *14*, 29.
(3) Bauer, D. R.; Brauman, J. J.; Pecora, R. *Macromolecules* **1975**, *8*, 443.
(4) Bendler, J. T.; Yaris, R. *Macromolecules* **1978**, *11*, 650.
(5) Helfand, E. *J. Chem. Phys.* **1971**, *54*, 4651.
(6) Blomberg, C. *Chem. Phys.* **1979**, *37*, 219.
(7) Fixman, M.; Evans, G. T. *J. Chem. Phys.* **1978**, *68*, 195.
(8) Adler, R. S.; Freed, K. F. *J. Chem. Phys.* **1980**, *72*, 2032.
(9) Weiner, J. H.; Pear, M. R. *Macromolecules* **1977**, *10*, 317.

(10) Helfand, E.; Wasserman, Z. R.; Weber, T. A. *Macromolecules* **1980**, *13*, 526.
(11) Fixman, M. *J. Chem. Phys.* **1979**, *69*, 1527, 1538.
(12) Robertas, D. W.; Berne, B. J.; Chandler, D. *J. Chem. Phys.* **1979**, *70*, 3397.
(13) Skolnick, J.; Helfand, E. *J. Chem. Phys.* **1980**, *72*, 5489.
(14) Flory, P. J. "Statistical Mechanics of Chain Molecules"; Interscience: New York, 1969.
(15) Herzberg, G. "Molecular Spectra and Molecular Structure"; Van Nostrand: New York, 1959; Vol. II.
(16) Houk, K. N., personal communication.
(17) The saddle point on the potential energy surface corresponds to the configuration $\mathbf{r}^* = (\mathbf{r}_1^* \ldots \mathbf{r}_N^*)$ in which all the bond lengths, bond angles, and nontransforming torsional angles are at potential minima and the single transforming rotational angle is at the top of the barrier between the trans and gauche states. In the vicinity of $\mathbf{r}^*$ the potential $V(\mathbf{r})$, defined relative to the conformation in which all the bond lengths, bond angles, and torsional angles are at potential minima, may be expanded about $\mathbf{r}^*$ to give

$$V(\mathbf{r}) = E^* + \tfrac{1}{2}\sum_{i,j=1}^{3N} W_{ij}(x_i - x_i^*)(x_j - x_j^*)$$

Note that since all the bond lengths, bond angles, and torsional angles associated with $\mathbf{r}^*$ are at potential extrema, the gradient of $V(\mathbf{r})$ evaluated at $\mathbf{r}^*$ must vanish. The potential matrix $\boldsymbol{W}$ has a single negative eigenvalue λ, whose eigenvector ρ^* points in the direction of the path of steepest descents. $\boldsymbol{W}$ is diagonalized numerically to give both λ and ρ^*.
(18) Gronski, W.; Murayama, N. *Makromol. Chem.* **1979**, *180*, 277.
(19) Broecker, H. C.; Klahn, J. *Makromol. Chem.* **1979**, *180*, 551.

Degradation of Chain Molecules. 1. Exact Solution of the Kinetic Equations†

M. Ballauff‡ and B. A. Wolf*

Institut für Physikalische Chemie der Universität Mainz, D-6500 Mainz, West Germany.
Received July 11, 1980

ABSTRACT: A general solution of the rate equations representing the degradation of chain molecules is given. The treatment can be applied to any set of equations and to any initial distribution. Model calculations are performed for random scission, for Gaussian probability of scission, and for scission exclusively at the midpoint of the chain. The starting molecular weight distribution is of the Schulz type, differing in the nonuniformity. The results clearly demonstrate that, by fitting the model parameters to experimental distributions, the full kinetic information concerning the degradation process is obtained.

Since the days of Staudinger,[1] it has been known that polymer chains can break due to high shear mechanical action. The cleavage of bonds by chemical attack, e.g., by hydrolysis, is also a well-investigated phenomenon.[2,3] A third possibility of degradation is by radiation-induced chain scission.[4,5]

The first theoretical treatments of these phenomena were given by Kuhn[6] and by Montroll and Simha,[7] who elaborated a statistical method to solve the problem of random scission. In this model it is assumed that the accessibility to cleavage is independent of the position of the bond in the chain. Furthermore, the starting material is taken to be uniform. Starting from Saito's integrodifferential equation,[8] Kotliar[9] and Inokuti and Dole[10] have derived expressions for the average molecular weights resulting from random scission. The starting molecular weight distribution is of the Schulz–Zimm type.[11] The problem of calculation of the entire molecular weight distribution (MWD) of the degraded polymers instead of different molecular weight averages only was studied by Kotliar[12] by means of a Monte Carlo approach. In order to solve this problem analytically, Jellinek and White elaborated a kinetic scheme,[13] which was refined by Mostafa[14] applying matrix algebra. Glynn, van der Hoff, and Reilly developed a numerical scheme to fit different theoretical breakage models, including nonrandom processes to experimental molecular weight distributions.[15] A set of equations describing the degradation process was given by Basedow, Ebert, and Ederer[3] and solved exactly for the case of random scission.

Over the past few years gel permeation chromatography has become a convenient and reliable method and it is now possible to measure not only the different molecular weight averages (M_n, M_w, M_z) but also the MWD of the degraded samples with sufficient accuracy in short time. Obviously knowledge of the change in the MWD throughout the degradation gives more insight into the mechanisms involved than that of the molecular weight averages as functions of time.

The general aim of a kinetic study is to obtain the individual rate constants k_i for the degradation of a species with degree of polymerization i and the individual rate constants $k_{i,j}$ for the scission of a chain of length i into two fragments with j and $i - j$ subunits, respectively. Clearly k_i is given by the sum over all $k_{i,j}$ of a molecule with i subunits

$$k_i = \sum_{j=1}^{i-1} k_{i,j} \tag{1}$$

There is one simple case where k_i can be obtained directly from the MWD, namely, if the molecules are essentially broken in the middle of the chain. Assuming this model, the reaction rates for the highest molecular weights present in the original sample can directly be determined by their disappearance in the degraded samples.

In all cases studied in this way so far,[16,17] the order of the reaction (dependence of the rate on the concentration of the i-mers) is 1. The disadvantage of this method lies in the fact that only a small part of the MWD can be treated in such a way. The obtainable insight into the mechanism of the degradation is therefore rather limited and the results may become quite uncertain. Consequently, one should apply a method which utilizes all information contained in the MWD and not only that of its

† Dedicated to Professor Dr. G. V. Schulz in honor of his 75th birthday.
‡ Part of the thesis of M. Ballauff.

0024-9297/81/2214-0654$01.25/0